Random Acoustic Response of a Cylindrical Shell

CHINTSUN HWANG* AND W. S. PI†
Northrop Corporation, Aircraft Division, Hawthorne, Calif.

The paper describes an analytical procedure to compute the spectral response of a cylindrical shell due to a random acoustic pressure input. In the general formulation, the pressure input may be both time-wise and space-wise random, while the computation is limited to a time-wise random pressure with definite spatial distribution. The analysis uses the modal approach to define the shell response. The interaction between the shell and the atmosphere is considered. Also considered are the shell structural damping as well as the air damping due to molecular absorption and dispersion. It is shown in the analysis that, in addition to the natural modes that are obtained by assuming a frictionless shell operating in a vacuum, the impedance of the air column inside the cylindrical shell plays a significant role in determining the random acoustic response of the shell. The paper also describes a formulation of the mean pressure spectrum inside the shell enclosure due to reverberation. Based on the analysis, spectral data are generated for two typical cylindrical shells under random acoustic excitation.

Nomenclature

a = radius of the cylindrical shell middle surface
a_{nqs},b_{nqs} = Fourier coefficients
$\bar{a}$ = $\Sigma\alpha A$ = shell wall absorption
A = $2\pi al$ = area
c = speed of sound in air
$c_{(s)}$ = speed of sound of the shell material
C_{on},C_{in} = functions related to acoustic impedance
E = Young's modulus of shell material
f = acoustic pressure distribution
$f(Hz)$ = $\omega/2\pi$ = frequency
F = effective load on the shell surface
g_1,g_2 = air damping constants
G = gravitational acceleration
h = shell thickness
H = transfer function
$\bar{k}_1$ = $[(1 - ig_1)(\omega/c)^2]^{1/2}$ = wave number, exterior of shell
$\bar{k}_2$ = $[(1 - ig_2)(\omega/c)^2]^{1/2}$ = wave number, interior of shell
$\bar{k}_{r1},\bar{k}_{r2}$ = acoustic wave numbers in the radial direction, exterior and interior of shell, respectively
$k_{(s)}$ = $\omega/c_{(s)}$ = shell wave number
K_1,K_2 = wave numbers of shell natural modes $K_1 = p\pi/l$, $K_2 = n/a$
l = length of the cylindrical shell
n,m = circumferential harmonic number
p,q = harmonic number along the shell meridian; q is also used to identify shell orthogonal modes $\alpha_{nq}(x)$ for the general case
p_i = internal pressure
p_0 = external pressure
$\bar{p}$ = rms value of the acoustic pressure in the enclosure over the volume
$p_{(s)}$ = internal pressure on the shell surface
r = radial coordinate
s = harmonic number of the Fourier components of the orthogonal mode $\alpha_{nq}(x)$
$S(\omega)$ = Fourier transform, the subscript indicates the function involved
$S^*(\omega)$ = conjugate of Fourier transform
t,T = time
V = volume
$w_n,\bar{w}_n$ = shell normal displacement components
w,W = shell normal displacement
$\dot{W}$ = shell normal velocity
x = coordinate along the cylindrical axis
$Y_n(\omega)$ = modal impedance
$Y_{n(s)}(\omega)$ = modal impedance of shell operating in a vacuum
$Y_{n(a)}(\omega)$ = modal impedance due to shell-air interaction
α = absorption coefficient
α_n,α_{nq} = shell natural mode
ϵ = $h/[12(1 - \nu^2)]^{1/2}a$ = modified thickness ratio
$\bar{\epsilon}$ = average energy density
ξ = displacement
Π = energy input rate
ρ = air density
$\rho_{(s)}$ = shell material density
τ = time
Υ = average wave intensity
φ = cylindrical angle
$\phi(\omega)$ = power spectrum; the subscript indicates the function involved
ω_n = shell natural frequencies
ω,Ω = circular frequencies
∇^2 = $\partial^2/\partial r^2 + (1/r)\partial/\partial r + (1/r^2)\partial^2/\partial\varphi^2 + \partial^2/\partial x^2$ = Laplace operator
$\nabla_{(s)}{}^2$ = $\partial^2/\partial x^2 + (1/a^2)\partial^2/\partial\varphi^2$ = Laplace operator on the cylindrical shell surface
(a) = function related to air
(s) = function related to shell

Received December 26, 1968; revision received June 5, 1969. Part of the work was carried out under Contract NAS8-20025, sponsored by the Vibration and Acoustics Branch, Structures Division, Propulsion and Vehicle Engineering Lab, NASA Marshall Space Flight Center.

* Manager, Structures and Dynamics Research Department. Associate Fellow AIAA.

† Engineering Specialist, Structures and Dynamics Research Department.

Introduction

IN engineering application, it is not uncommon to subject a shell structure to intense acoustic pressure. The pressure input to the shell may be either time-wise random or both time-wise and space-wise random. The response of the shell to such pressure is very complicated because of the nature of the excitation as well as the multiplicity of the natural modes of the shell structure along the frequency band of interest. The experimental data of the shell responses are usually presented in the form of power spectra. In order to put the spectral data in a manageable format, the common approach has been to process the data using a filter of finite band width (e.g., one-third octave band). The resulting step-wise spectral data are evaluated against similar data generated through an analytical procedure where the modal density of the structure (i.e., the number of natural modes in a certain frequency band) is used as a basis to determine the approximate spectral amplitude in the frequency band.

The aforementioned analytical method of processing the shell response spectra using the modal density approach is essentially an averaging technique. It is usable to establish a general spectral pattern of the shell response along the frequency band. It cannot handle the spectral details such as individual peaks and valleys of narrow width that appear often in the power spectra of a lightly-damped shell structure. The present paper represents an effort to establish the spectral details through individual consideration of each natural mode.

Specifically, the paper deals with the random acoustic excitation of a simply-supported cylindrical shell. An eighth-order differential equation is used to calculate the Fourier transform of the shell modal response due to the random pressure input. The interaction between the shell and the surrounding atmosphere is taken into consideration through the use of the acoustic field equations. The power spectra of the shell responses are organized using the Fourier transform data. This spectral formulation follows the general scheme used by Rice,[1] Powell,[2,3] and other investigators. Related works on cylindrical shell acoustic excitation may be found in Refs. 4 and 5.

Analytical Formulation

Consider a cylindrical shell operating in the atmosphere. A random acoustic pressure is applied on the shell outer surface. The shell responds to the excitation. The normal displacement of the vibrating shell causes a corresponding movement of the air on both sides of the shell. As a result, pressure impedances are generated which are felt by the shell. The objective of the analysis is to obtain the shell response spectra due to a specified random pressure input. In order to simplify the problem, the following assumptions are made.

1) The shell response may be resolved in terms of natural modes of a frictionless but otherwise identical shell operating in a vacuum.

2) The shell is sufficiently thin and the strain energy due to bending dominates. The in-plane displacements, even though considered in the shell dynamic analysis, are ignored in setting up the shell-air interaction boundary conditions.

3) The air impedance may be generated based on three-dimensional acoustic field equations using linearized boundary conditions.

4) The air inside the cylindrical shell is isolated from the external atmosphere except through shell vibration. The two ends of the shell are bounded by rigid plates. The reverberation effect of the shell enclosure is not considered in the shell response computation.

In the following sections, the impedances of the air inside and outside of the cylindrical shell are established. The shell dynamic equation is formulated including the air impedance functions. The resulting modal solution of the shell dynamic equation in the frequency domain serves as a basis to generate the shell response power spectra corresponding to a given random acoustic pressure input.

Air Impedance

Consider the external pressure change in the immediate neighborhood of the cylindrical shell due to shell motion. The acoustic wave propagation equation in cylindrical coordinates is

$$\nabla^2 p(r,\varphi,x,t) = (1/c^2)(\partial^2 p/\partial t^2 + g_1\omega\partial p/\partial t) \quad (1)$$

where

$$\nabla^2 = \partial^2/\partial r^2 + (1/r)\partial/\partial r + (1/r^2)\partial^2/\partial\varphi^2 + \partial^2/\partial x^2$$

and g_1 is the air damping coefficient due to molecular absorption, dispersion, and viscosity.[6] The linearized boundary condition at $r = a$ is

$$(\partial p/\partial r)(a,\varphi,x,t) = -\rho(\partial \dot{W}/\partial t)(\varphi,x,t) \quad (2)$$

Excluding the breathing mode, the cylindrical shell motion may be represented as

$$W(\varphi,x,t) = \sum_n \alpha_n(x)[w_n(t)\cos n\varphi + \bar{w}_n(t)\sin n\varphi] \quad (3)$$

$$n = 1,2,3,\ldots$$

In order to simplify the expressions without loss in generality, the terms involving $\bar{w}_n(t)$ will be omitted in the analysis. It is also understood that there may be more than one mode $w_n(t)\alpha_n(x)$ for a single n, in which case, the various α_n's are orthogonal to each other. For simply-supported cylindrical shell, Eq. (3) may be written as

$$W(\varphi,x,t) = \sum_n\sum_p w_{np}(t)\sin\frac{p\pi x}{l}\cos n\varphi \quad (4)$$

$$n,\ p = 1,2,3,\ldots$$

where x is measured from one end of the cylindrical shell. In the following, the more general expression (3) without $\bar{w}_n$ terms is used for simplicity as well as for the fact that the response power spectrum formulation is not limited to a simply-supported cylindrical shell. Equation (4) is used in the numerical computation at the end of the paper.

The aforementioned Eqs. (1–3) may be combined to yield the external pressure field of the cylindrical shell. Thus, the Fourier transform of Eq. (1) is

$$\nabla^2 S_p(r,\varphi,x,\omega) = -\bar{k}_1^2 S_p(r,\varphi,x,\omega) \quad (5)$$

where $\bar{k}_1 = [(1 - ig_1)(\omega/c)^2]^{1/2}$. For random pressure distribution $p(r,\varphi,x,\omega)$, it is understood that S_p indicates a Fourier type transform of the pressure with the integration carried out along a large time interval $(-T,T)$. Furthermore, S_p may be expanded into a series as follows:

$$S_p(r,\varphi,x,\omega) = \sum_n S_{pon}(r,x,\omega)\cos n\varphi \quad (6)$$

Based on Eqs. (2, 3, and 5), it may be shown that

$$S_{pon}(r,x,\omega) = -\frac{2\rho\omega^2}{\bar{k}_{r1}}\frac{\alpha_n(x)H_n^{(2)}(\bar{k}_{r1}r)}{[H_{n+1}^{(2)}(\bar{k}_{r1}a) - H_{n-1}^{2}(\bar{k}_{r1}a)]}S_{w_n}(\omega) \quad (7)$$

where $H_n^{(2)}(\bar{k}_{r1}r)$ is the Hankel's function of the second kind and of order n, and $\bar{k}_{r1} = (\bar{k}_1^2 - K_1^2)^{1/2}$ is the acoustic wave number along the radial direction. Equation (7) applies only when $\alpha_n(x)$ has a single wave number K_1. For a more general case, $\alpha_n(x)$ may be resolved into a number of components. Corresponding to each component term, a corresponding pressure response term of the type of Eq. (7) exists. The sum of the terms make up the total pressure response.

A somewhat similar expression may be established for the interior of a vibrating cylindrical shell. Thus, the Fourier transform of the pressure inside the cylindrical enclosure is

$$S_{pin}(r,x,\omega) = -\frac{2\rho\omega^2}{\bar{k}_{r2}}\frac{\alpha_n(x)J_n(\bar{k}_{r2}r)}{[J_{n+1}(\bar{k}_{r2}a) - J_{n-1}(\bar{k}_{r2}a)]}S_{w_n}(\omega) \quad (8)$$

where $\bar{k}_{r2} = [\bar{k}_2^2 - K_1^2]^{1/2}$, and g_2 is the air damping coefficient. The phase shift due to friction g_2 between the pressure component $S_{pin}(a,x,\omega)$ and the shell velocity component $\alpha_n S_{\dot{w}_n}$ determines the energy input rate $\Pi(\omega)$ to the enclosed air. As will be shown later in the equation of reverberation, the internal pressure power spectrum is dependent on the energy input rate.

Shell Dynamic Equation

The cylindrical shell dynamic equation is

$$\left[(1 + ig_{(s)})\left(\epsilon^2\nabla_{(s)}{}^8 + \frac{1}{a^4}\frac{\partial^4}{\partial x^4}\right) + \frac{1}{c_{(s)}{}^2a^2}\frac{\partial^2}{\partial t^2}\nabla_{(s)}{}^4\right]W(\varphi,x,t) = \frac{1}{Eha^2}\nabla_{(s)}{}^4F(\varphi,x,t) \quad (9)$$

where $\nabla_{(s)}{}^2 = \partial^2/\partial x^2 + (1/a^2)\partial^2/\partial\varphi^2$ and the structural damping constant is $g_{(s)}$. Equation (9) is a version of the Vlasov shell equation.[7] The equation considers the in-plane and normal deformations of the shell elements and the related continuity conditions, whereas the in-plane inertia forces are ignored. The external load $F(\varphi,x,t)$ normal to the shell surface includes the random acoustic pressure as well as the induced pressures due to shell motion. It has been assumed that W may be represented in terms of the normal modes, Eq. (3) or (4). For the general case of orthogonal shell modes $\alpha_n(x)$, Eq. (9) is applicable by resolving the modal pattern $\alpha_n(x)$ into Fourier components. For simplicity in presentation, the remainder part of the section will describe the special case of the simply-supported cylindrical shell, Eq. (4). At the end, the corresponding shell response function for the general case will be described.

For the simply supported case, two wave numbers (K_1, K_2) exist for each mode of W. Corresponding to each mode, the Laplace operator performed on W yields

$$\nabla_{(s)}{}^2W = -(K_1{}^2 + K_2{}^2)W = -(p^2\pi^2/l^2 + n^2/a^2)W \quad (10)$$

The Fourier transform of F is

$$S_F(\varphi,x,\omega) = -S_f(\varphi,x,\omega) - \sum_n S_{pon}(a,x,\omega)\cos n\varphi + \sum_n S_{pin}(a,x,\omega)\cos n\varphi \quad (11)$$

where S_f represents the limiting function of the Fourier transform of the random acoustic pressure load and S_{pon} and S_{pin} are given in Eqs. (7) and (8).

Making use of Eqs. (10) and (11), the Fourier transform of Eq. (9) is

$$\sum_n\left[(1 + ig_{(s)})\frac{\omega_n{}^2}{c_{(s)}{}^2a^2}\left(\frac{p^2\pi^2}{l^2} + \frac{n^2}{a^2}\right)^2 - \frac{k_{(s)}{}^2}{a^2}\left(\frac{p^2\pi^2}{l^2} + \frac{n^2}{a^2}\right)^2 + \frac{k_{(s)}{}^2}{a^2}\left(\frac{\rho}{\rho_{(s)}}\right)\left(\frac{a}{h}\right)\left(\frac{p^2\pi^2}{l^2} + \frac{n^2}{a^2}\right)^2(-C_{on} + C_{in})\right] \times S_{wn}(\omega)\alpha_n(x)\cos n\varphi = -\frac{1}{Eha^2}\nabla_{(s)}{}^4S_f(\varphi,x,\omega) \quad (12)$$

where

$$\omega_n{}^2 = c_{(s)}{}^2a^2\left[\epsilon^2\left(\frac{p^2\pi^2}{l^2} + \frac{n^2}{a^2}\right)^2 + \frac{p^4\pi^4/l^4}{a^4(p^2\pi^2/l^2 + n^2/a^2)^2}\right] \quad (13)$$

$$C_{on}(\bar{k}_{r1}a) = \frac{2}{\bar{k}_{r1}a}\frac{H_n{}^{(2)}(\bar{k}_{r1}a)}{[H_{n+1}{}^{(2)}(\bar{k}_{r1}a) - H_{n-1}{}^{(2)}(\bar{k}_{r1}a)]} \quad (14)$$

$$C_{in}(\bar{k}_{r2}a) = \frac{2}{\bar{k}_{r2}a}\frac{J_n(\bar{k}_{r2}a)}{[J_{n+1}(\bar{k}_{r2}a) - J_{n-1}(\bar{k}_{r2}a)]} \quad (15)$$

It is noted that $C_{on}(\bar{k}_{r1}a)$, $C_{in}(\bar{k}_{r2}a)$ are dependent on the acoustic wave numbers $\bar{k}_1,\bar{k}_2$, the circumferential harmonic number n, and the shell axial wave number K_1. Again, the modal summation sign for various p's corresponding to a given n is omitted in Eq. (12) to simplify the presentation. For the special case of $g_2 = 0$, i.e., damping not considered, $C_{in}(\bar{k}_{r2}a)$ is a real function of the nondimensional frequency. The impedance approaches infinity at frequencies where $J'_n(\bar{k}_{r2}a) = 0$. It is noted that these frequencies are identical to the nth cutoff frequencies for sound transmission in a cylindrical pipe.[8] The impedance function is modified with the introduction of nonzero damping constant g_2. As will be shown in the numerical example, the attenuation is most prominent in the neighborhood of the nth cutoff frequencies.

Equation (12) may be simplified through surface integration using the orthogonal properties. The equation yields the Fourier transform of the modal response due to random excitation S_f:

$$S_{wn}(\omega) = \frac{1}{Y_n(\omega)}\int_0^{2\pi}\int_0^l \frac{\nabla_{(s)}{}^4S_f(\varphi,x,\omega)}{(p^2\pi^2/l^2 + n^2/a^2)^2}\alpha_n(x)\cos n\varphi\, dx\, d\varphi \quad (16)$$

where $Y_n(\omega)$ is the shell modal impedance

$$Y_n(\omega) = -\pi\rho_{(s)}h\int_0^l \alpha_n{}^2(x)dx\left\{(1 + ig_{(s)})\omega_n{}^2 - \omega^2 - \frac{\rho}{\rho_{(s)}}\frac{a}{h}\omega^2[C_{on}(\bar{k}_{r1}a) - C_{in}(\bar{k}_{r2}a)]\right\} \quad (17)$$

On the right-hand side of Eq. (17), the first term inside the parentheses represents the contribution due to shell stiffness. The second term represents the contribution due to the inertia of the shell material. The last two terms involving $C_{on}(\bar{k}_{r1}a)$ and $C_{in}(\bar{k}_{r2}a)$ are the impedances due to shell-air interaction. For each mode, the relative importance of the impedances due to shell-air interaction as against that due to shell inertia may be evaluated through the following quantity:

$$[\rho/\rho_{(s)}](a/h)[C_{on}(\bar{k}_{r1}a) - C_{in}(\bar{k}_{r2}a)]$$

For the general case of a shell with orthogonal modes $\alpha_{nq}(x)$ corresponding to a given circumferential harmonic number n, each mode $\alpha_{nq}(x)$ may be resolved into the Fourier components as shown below:

$$\alpha_{nq}(x) = \sum_s\left[a_{nqs}\cos\frac{s\pi x}{2l} + b_{nqs}\sin\frac{s\pi x}{2l}\right] \quad (18)$$

It can be shown that the corresponding limit function of the Fourier transform of the shell response due to random pressure excitation is

$$S_W(\varphi,x,\omega) = \sum_n\sum_q \alpha_{nq}(x)\cos n\varphi \sum_s \times \frac{1}{Y_{nqs}(\omega)}\int_0^{2\pi}\int_0^l \frac{\nabla_{(s)}{}^4S_f(\varphi,x,\omega)}{(s^2\pi^2/4l^2 + n^2/a^2)^2}\left(a_{nqs}\cos\frac{s\pi x}{2l} + b_{nqs}\sin\frac{s\pi x}{2l}\right)\cos n\varphi\, dx\, d\varphi \quad (19)$$

where

$$Y_{nqs}(\omega) = -\pi\rho_{(s)}h\int_0^l \alpha_{nq}{}^2(x)dx\left\{(1 + ig_{(s)})c_{(s)}{}^2a^2 \times \left[\epsilon^2\left(\frac{s^2\pi^2}{4l^2} + \frac{n^2}{a^2}\right)^2 + \frac{(s\pi/2l)^4}{a^4}\left(\frac{s^2\pi^2}{4l^2} + \frac{n^2}{a^2}\right)^{-2}\right] - \omega^2 - \frac{\rho}{\rho_{(s)}}\frac{a}{h}\omega^2[C_{on}(\bar{k}_{rs1}a) - C_{in}(\bar{k}_{rs2}a)]\right\} \quad (20)$$

and

$$\bar{k}_{rs1} = (\bar{k}_1{}^2 - s^2\pi^2/4l^2)^{1/2},\quad \bar{k}_{rs2} = (\bar{k}_2{}^2 - s^2\pi^2/4l^2)^{1/2}$$

Shell Response Power Spectrum

Following the approach used by Powell,[3] the shell response power spectrum may be obtained by taking the limit of the complex conjugate product of the Fourier transforms. Thus, for the simply supported shell, the response spectrum is

$$\phi_W(\varphi,x,\omega) = \sum_n \sum_m \frac{\alpha_n(x)\alpha_m(x)\cos n\varphi \cos m\varphi}{Y_n(\omega)Y_m^*(\omega)} \cdot \int_0^{2\pi}\int_0^l\int_0^{2\pi}\int_0^l \lim_{T\to\infty} \frac{1}{T} \frac{\nabla_{(s)}{}^4 S_f(\varphi,x,\omega)}{(p^2\pi^2/l^2 + n^2/a^2)^2} \times \frac{\nabla_{(s)}{}^4 S_f^*(\varphi',x',\omega)}{(q^2\pi^2/l^2 + m^2/a^2)^2} \alpha_n(x) \cos n\varphi \alpha_m(x') \cos m\varphi' dx d\varphi dx' d\varphi' \quad (21)$$

Equation (21) indicates the dependence of the shell response power spectrum on the modal impedance $Y_n(\omega)$ and the acoustic pressure $S_f(\varphi,x,\omega)$. In the equation, area integration is carried out on $\nabla_{(s)}{}^4 S_f(\varphi,x,\omega)$. The result of the integration is a generalized function of $\nabla_{(s)}{}^4 S_f(\varphi,x,\omega)$ corresponding to a natural mode $\alpha_n(x)\cos n\varphi$. The generalized function is to be multiplied by a factor of the order ω_n^{-2} $(p^2\pi^2/l^2 + n^2/a^2)^{-2}$ to form a typical term of the series in Eq. (21). It can be shown that for various spatial distributions of $S_f(\varphi,x,\omega)$, the resulting double series of Eq. (21) converge absolutely. As a result, the truncation of the double series in the response spectral computation is justified.

Reverberation Effect

In the preceding analysis, the pressure exerted by the air inside the cylindrical shell is somewhat out of phase with respect to the shell displacement due to air friction, Eq. (8). As a result, work is done to the internal air by the shell which results in a pressure buildup. In reality, as the internal acoustic pressure wave impinges on the shell, the majority of the wave energy is reflected back to the air. A small percentage is absorbed by the shell wall. A balance is maintained in the energy transfer as well as the internal acoustic pressure level. The resulting effect, called reverberation, may be analyzed using energy equilibrium equations. According to Morse,[8] the average acoustic energy density in volume V is

$$\bar{\epsilon}(t) = \frac{\rho}{2V}\int_V \left[\left|\frac{\partial \xi}{\partial t}\right|^2 + c^2(\nabla\cdot\xi)^2\right] dV = \frac{1}{\rho c^2}\bar{p}^2(t) \quad (22)$$

where $\nabla\cdot\xi$ indicates the spatial gradient of the displacement and $\bar{p}^2(t)$ is the square of the average acoustic pressure in the enclosure. The acoustic wave intensity, i.e., the rate of acoustic energy transmission per unit area, is related to the energy density by the following relation:

$$\Upsilon(t) = (c/4)\bar{\epsilon}(t) = (1/4\rho c)\bar{p}^2(t) \quad (23)$$

The total energy input rate to the enclosure due to shell motion is

$$\Pi(t) = -\frac{1}{2} Re \int_A p_{(s)}(t)\dot{W}^*(t) dA \quad (24)$$

where $\dot{W}^*(t)$ indicates the conjugate of the shell normal velocity $\dot{W}$, and the negative sign accounts for the fact that the pressure is applied to the air in a direction opposite to $\dot{W}$. In a reverberation chamber, part of the acoustic energy transmitted toward the wall is reflected back to the enclosed air. The remaining portion is absorbed by the wall. The absorption of the wall is defined as $\bar{a} = \Sigma\alpha A$, i.e., percentage absorption times area. The energy balance inside the enclosure with a moving wall is represented by the following equation:

$$(d/dt)[4V\Upsilon(t)/c] = \Pi(t) - \bar{a}\Upsilon(t) \quad (25)$$

The solution of Eq. (25) is

$$\Upsilon(t) = \frac{c}{4V} e^{-(\bar{a}c/4V)t} \int_{-\infty}^{t} e^{(\bar{a}c/4V)\tau}\, \Pi(\tau) d\tau \quad (26)$$

Both sides of Eq. (26) are integrated with respect to time to obtain a time-wise mean value. After the averaging

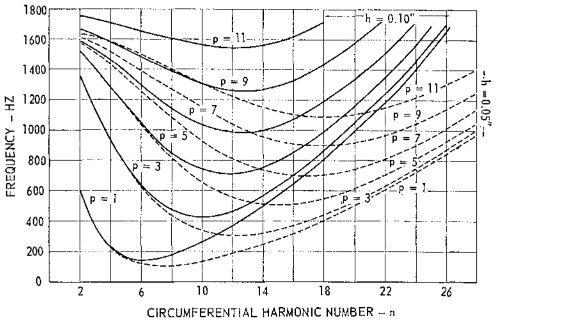

Fig. 1 Natural frequencies of the simply-supported cylindrical shells.

process, the left-hand side (LHS) is

$$LHS = \lim_{T\to\infty} \frac{1}{2T}\int_{-T}^{T} \Upsilon(t) dt = \frac{1}{4\rho c}\overline{\bar{p}^2(t)} = \frac{1}{4\rho c}\int_0^\infty \Phi_{\bar{p}}(\omega) d\omega \quad (27)$$

where use has been made of Eq. (23). Applying the same procedure, the right-hand side (RHS) of Eq. (26) is

$$RHS = \frac{1}{\bar{a}} \lim_{T\to\infty} \frac{1}{2T} \times \left\{ -\left[e^{-(\bar{a}c/4V)t} \int_{-\infty}^{t} e^{(\bar{a}c/4V)\tau}\, \Pi(\tau) d\tau \right]_{t=-T}^{t=T} + \int_{-T}^{T} e^{-(\bar{a}c/4V)t} e^{(\bar{a}c/4V)t}\, \Pi(t) dt \right\} \quad (28)$$

It can be shown that in the limiting case, the first term in the parentheses of Eq. (28) vanishes. Applying Eq. (24) to the remaining term, the following is reached:

$$\begin{aligned} RHS &= \frac{1}{\bar{a}} \lim_{T\to\infty} \frac{1}{2T}\int_{-T}^{T} \Pi(t) dt \\ &= -\frac{1}{\bar{a}} \lim_{T\to\infty} \frac{1}{2T}\int_{-T}^{T} \frac{1}{2} Re \int_A P_{(s)}(t)\dot{W}^*(t) dA dt \\ &= -\frac{1}{4\pi\bar{a}}\int_A \lim_{T\to\infty}\frac{1}{2T} Re \int_{-T}^{T}\int_{-\infty}^{\infty} S_{p(s)}(\omega)e^{i\omega t} d\omega \times \int_{-\infty}^{\infty} S_{\dot{W}}^*(\omega')e^{-i\omega' t}\, d\omega' dt dA \\ &= -\frac{1}{2\bar{a}}\int_A \lim_{T\to\infty}\frac{1}{2T} Re \int_{-\infty}^{\infty}\int_{-\infty}^{\infty} S_{p(s)}(\omega) S_{\dot{W}}^*(\omega') \times \delta(\omega - \omega') d\omega' d\omega dA \\ &= -\frac{1}{\bar{a}}\int_0^\infty \lim_{T\to\infty}\frac{1}{2T} Re \int_A S_{p(s)}(\omega) S_{\dot{W}}^*(\omega) dA d\omega \end{aligned} \quad (29)$$

Combining Eqs. (27) and (29) yields the rms pressure inside the shell enclosure

$$\bar{p}^2 = \int_0^\infty \phi_{\bar{p}}(\omega) d\omega = -\frac{4\rho c}{\bar{a}}\int_0^\infty \lim_{T\to\infty}\frac{1}{2T} \times Re \int_A S_{p(s)}(\omega) S_{\dot{W}}^*(\omega) dA d\omega \quad (30)$$

Consider the case where the enclosure acoustic response is a linear function of the input in the frequency domain, i.e., no subharmonics of the acoustic field are generated due to a single frequency excitation of the shell. Under this condition, the pressure spectral density may be resolved based on Eq. (30) as shown below:

$$\phi_{\bar{p}}(\omega) = -\frac{4\pi a\rho c}{\bar{a}} \sum_n \int_0^l \alpha_n^2(x) dx \lim_{T\to\infty} \frac{1}{2T} Re S_{pn}(\omega) S_{\dot{w}n}^*(\omega) \quad (31)$$

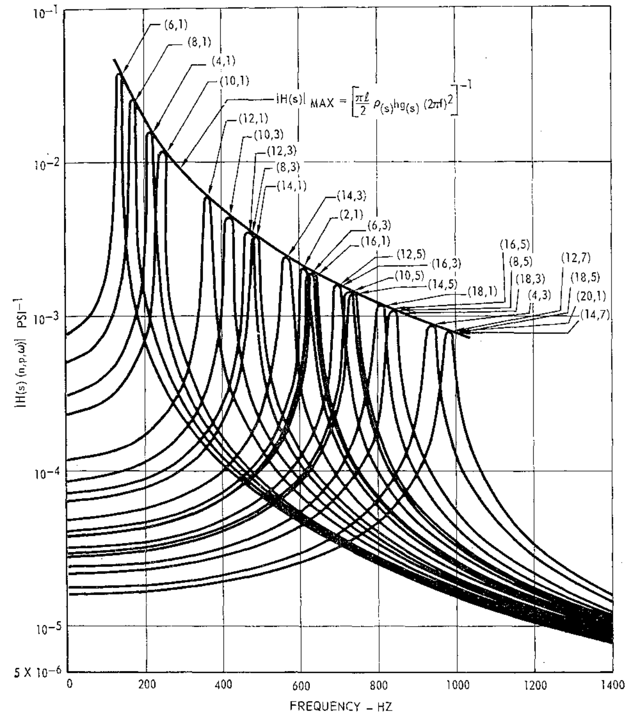

Fig. 2 Modal transfer functions of cylindrical shell 1 ignoring shell-air interaction.

In Eq. (31), the Fourier transform of the normal pressure $S_{p_n}(\omega)$ may be obtained from Eq. (8)

$$S_{p_n}(\omega) = -\frac{\rho\omega^2 a}{\bar{k}_{r2}a} \frac{J_n(\bar{k}_{r2}a)}{\frac{1}{2}[J_{n+1}(\bar{k}_{r2}a) - J_{n-1}(\bar{k}_{r2}a)]} S_{w_n}(\omega) \quad (32)$$

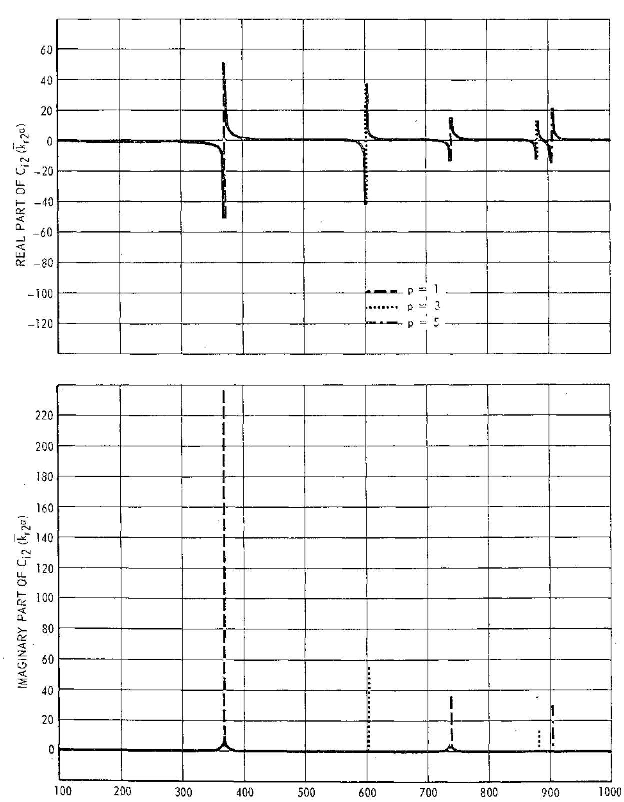

Fig. 3 Typical modal impedance function due to air inside the cylindrical shell.

so that

$$\bar{p}(\omega) = \frac{4\pi\rho^2\omega^2 a^2 c}{\bar{a}} \sum_n \int_0^l \alpha_n^2(x)dx \lim_{T\to\infty} \frac{1}{2T} \times Re\left\{\frac{1}{\bar{k}_{r2}a} \frac{J_n(\bar{k}_{r2}a)}{\frac{1}{2}[J_{n+1}(\bar{k}_{r2}a) - J_{n-1}(\bar{k}_{r2}a)]} S_{w_n}(\omega) S_{\dot{w}_n}{}^*(\omega)\right\}$$
$$= \frac{2\pi\rho^2\omega^3 a^2 c}{\bar{a}} \sum_n \int_0^l \alpha_n^2(x)dx Im[C_{in}(\bar{k}_{r2}a)]\phi_{w_n}(\omega) \quad (33)$$

where $\phi_{w_n}(\omega)$ is the shell displacement power spectrum at $(0,l/2)$ if only one shell mode $w_n\alpha_n$ exists. Equation (33) illustrates the dependence of the shell internal pressure spectral density to the shell modal data as well as the physical properties of the shell and the enclosed air.

Numerical Example

Consider two simply-supported cylindrical shells of the following dimensions and properties: 1) a = 20.0 in., l = 40.0 in., h = 0.10 in., $E = 10.3 \times 10^6$ psi, ν = 0.33, $\rho_{(s)}$ = 0.000259 lb sec^2/in.^{4}, $g_{(s)}$ = 0.02; 2) same as 1 except that h = 0.05 in.

The surrounding air has the following properties: $\rho_{(a)} = 0.1211 \times 10^{-6}$ lb sec^2/in.^{4}, $c_{(a)}$ = 1128 fps, $g_1 = g_2$ = 0.00122. Ignoring damping coefficient $g_{(s)}$, the natural frequencies of the two shells operating in a vacuum are first computed for various harmonic numbers (n,p) based on Eq. (13). The results are plotted in Fig. 1. Referring to the figure, certain combinations of (n,p,ω) will result in $\bar{k}_{r1} = (\bar{k}_1^2 - K_1^2)^{1/2}$, where $\bar{k}_{r1}$ is the square root of a complex number with a negative real part and a small imaginary part. Physically, the case represents a highly damped wave motion due to a large shell axial wave number and a relatively small acoustic wave number. Similar cases apply to $\bar{k}_{r2}$. These combina-

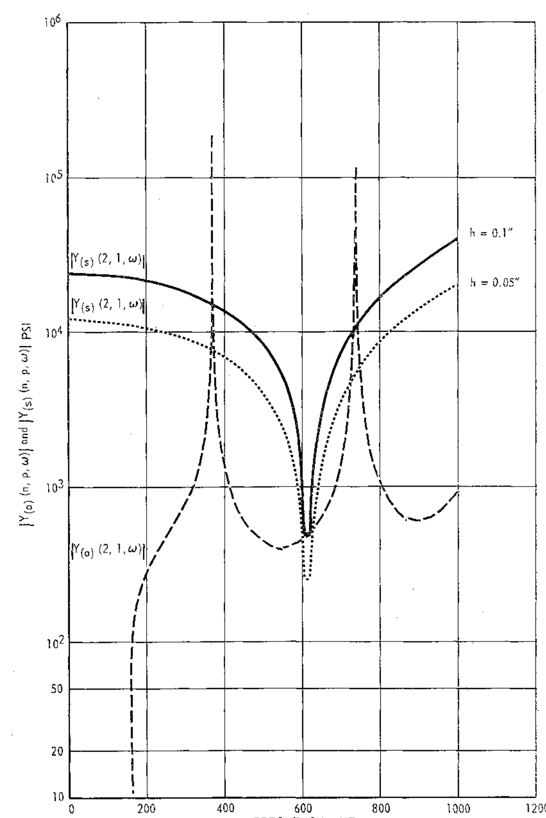

Fig. 4 Magnitude comparison of modal impedances due to shell operating in a vacuum and shell-air interaction.

tions are dropped in air impedance computations (7) and (8) because the corresponding wave motion cannot be sustained by a vibrating shell. A white noise with the following spatial distribution is applied on both shells:

$$\phi_f(\varphi,x,\omega) = \cos^2\varphi \text{ psi}^2/\text{Hz}, \; -\pi/2 \leq \varphi \leq \pi/2$$

$$\phi_f(\varphi,x,\omega) = 0, \; \pi/2 < \varphi < 3\pi/2$$

It is required to compute the shell acceleration spectra at selected location up to a frequency of 1000 Hz using a digital computer. Before going into the shell spectral data, it is worthwhile to analyze the modal impedance terms and their contributions to the over-all spectral response. Referring to Eqs. (16) and (17), the complex shell impedance function may be divided into two parts. The first part is the shell impedance when operated in a vacuum. The second part is the additional impedance due to shell-air interaction;

$$Y_n(\omega) = Y_{n(s)}(\omega) + Y_{n(a)}(\omega) \qquad (34)$$

$$Y_{n(s)}(\omega) = Y_{(s)}(n,p,\omega) = -\pi\rho_{(s)}h \int_0^l \alpha_n{}^2(x)dx[(1 + ig_{(s)})\omega_n{}^2 - \omega^2] \qquad (35)$$

$$Y_{n(a)}(\omega) = Y_{(a)}(n,p,\omega) = \pi\rho a\omega^2 \int_0^l \alpha_n{}^2(x)dx[C_{on}(\bar{k}_{r1}a) - C_{in}(\bar{k}_{r2}a)] \qquad (36)$$

Impedance terms (35) and (36) are computed separately. Typical data obtained in this manner are plotted in Figs. 2–5. Figure 2 shows the transfer function for shell 1 when $Y_{n(a)}(\omega)$ vanishes;

$$H_{(s)}(n,p,\omega) = 1/Y_{n(s)}(\omega) \qquad (37)$$

The absolute value of $H_{(s)}(n,p,\omega)$ is plotted against the frequency coordinate for a number of harmonic numbers (n,p). Figure 3 is a plot of $C_{in}(\bar{k}_{r2}a)$ where $n = 2$. It shows that for small g_2, both the real and imaginary parts of $C_{in}(\bar{k}_{r2}a)$ have significant contribution to the shell over-all impedance

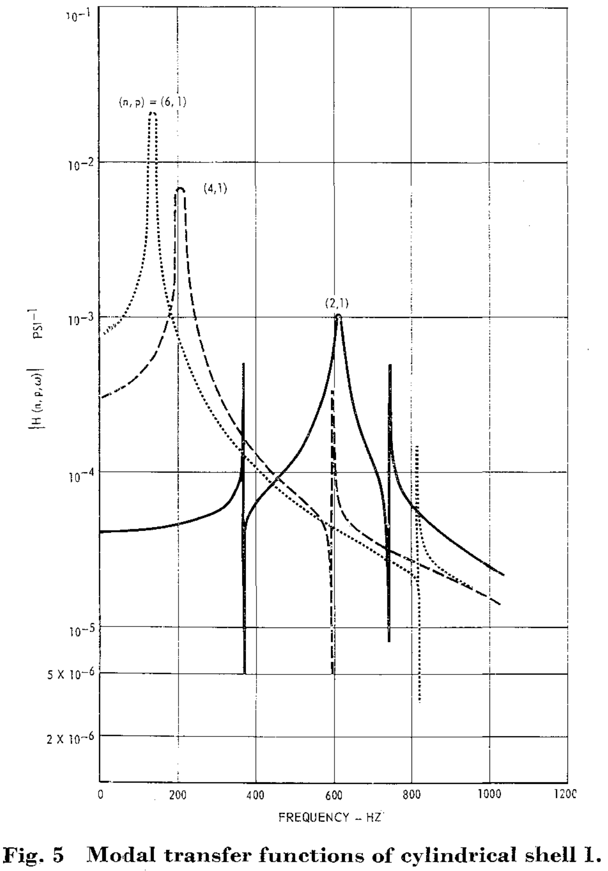

Fig. 5 Modal transfer functions of cylindrical shell 1.

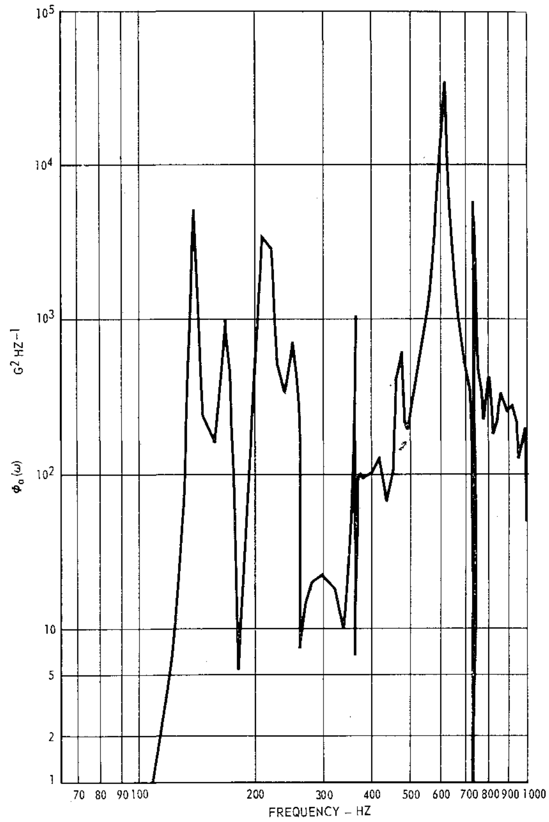

Fig. 6 Power spectrum of acceleration, cylindrical shell 1 at $(\varphi,x) = (0, l/2)$.

$Y_n(\omega)$ only in the immediate neighborhood of the nth cutoff frequencies, i.e., frequencies at which $J'_n(\bar{k}_{r2}a) = 0$ if $g_2 = 0$.

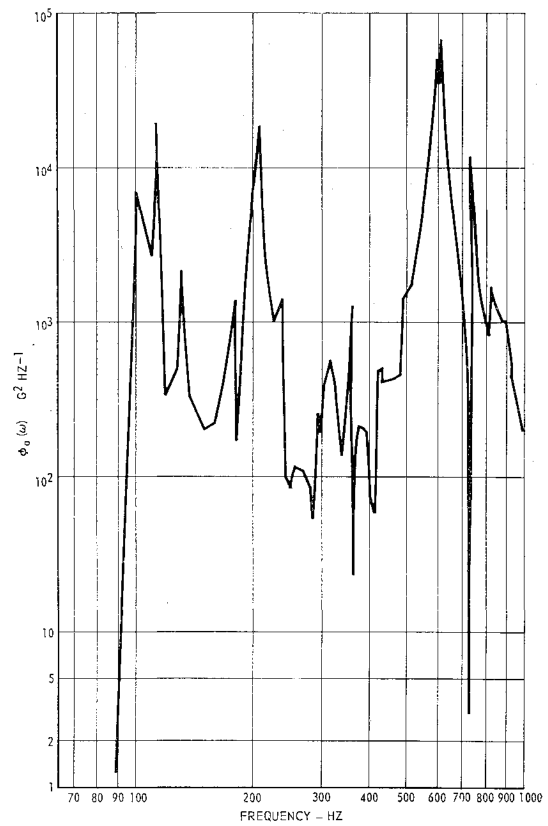

Fig. 7 Power spectrum of acceleration, cylindrical shell 2 at $(\varphi,x) = (0, l/2)$.

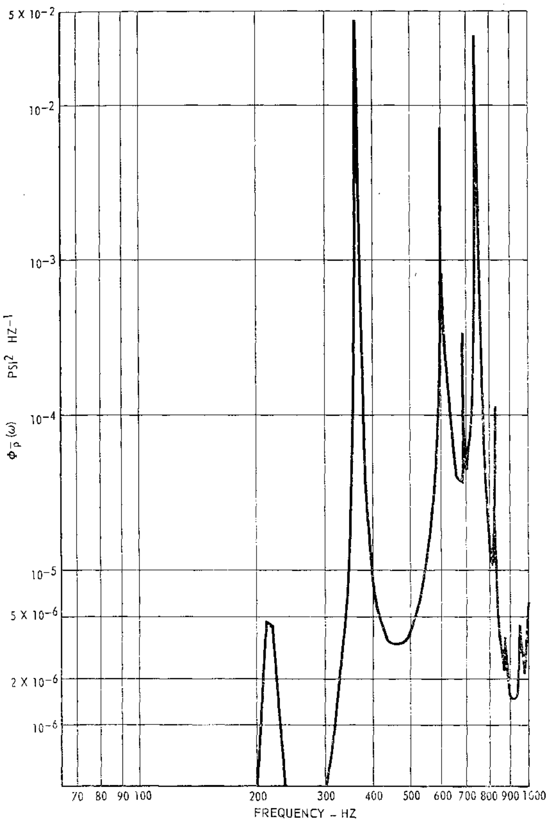

Fig. 8 Power spectrum of mean acoustic pressure inside cylindrical shell 1.

As will be shown later, the magnitude of $Y_{n(a)}(\omega)$ at a cutoff frequency is such that it may be reflected as a prominent valley in the shell response power spectrum. In Fig. 4, $|Y_{(a)}(n,p,\omega)|$ is plotted together with $|Y_{(s)}(n,p,\omega)|$ for $(n,p) = (2,1)$ for the two shells. From the figure, the significant contribution of $Y_{n(a)}(\omega)$ to $Y_n(\omega) = Y(n,p,\omega)$ is self-evident. Figure 5 shows the absolute value of the transfer function $H(n,p,\omega)$ of shell 1 which is the reciprocal of $Y(n,p,\omega)$ for typical harmonic numbers $(n,p) = (2,1)$, $(4,1)$, and $(6,1)$.

Based on Eq. (21) and applying the input pressure spectral distribution, it can be shown that for a finite ω, a typical term in each of the finite series is of the order of $\omega_n^{-2}(n^2/a^2)(p^2\pi^2/l^2 + n^2/a^2)^{-2}$ corresponding to increasing n,p. The series converges absolutely. Using Eq. (21), and the relationship between displacement and acceleration, the shell acceleration spectrum is computed in terms of G levels:

$$\phi_a(\omega) = (\omega^4/G^2)\phi_W(\omega) \tag{38}$$

Figure 6 is for $\phi_a(\omega)$ of shell 1 at $(\varphi,x) = (0,l/2)$. Figure 7 gives the acceleration spectrum of shell 2 at $(\varphi,x) = (0,l/2)$. The effect of the shell thickness on the shell response power spectrum may be observed from Eqs. (13, 17, and 18). Generally speaking, the level of the power spectral density of the shell response is roughly proportional to h^{-2}. The location of the peaks which reflect the shell natural modes varies with the shell thickness in the frequency domain, while the positions of the prominent valleys corresponding to the cutoff frequencies remain unchanged. Referring to Figs. 6 and 7, it may be seen that, in the frequency range between 100 and 135 Hz, shell 2 has three major peaks corresponding to the natural modes $(n,p) = (6,1)$, $(8,1)$, and $(10,1)$, whereas shell 1 has no peak at all, as may be evidenced in Fig. 2. Also, the over-all level of ϕ_a of shell $2(h = 0.05$ in.) is approximately four times higher than that of shell $1(h = 0.1$ in.). The latter fact confirms the statement that the shell response spectrum is approximately proportional to h^{-2}.

In order to test the rate of convergence of the infinite series in Eq. (21), the spectral data are computed for shell 1 using various numbers of truncated terms corresponding to the natural modes. It is found that the spectral density shows an increase of 2.4% at 1000 Hz, when the number of modes used in computation is increased from 40 to 112. The increase in spectral density in the lower frequency region is substantially less due to the additional modes considered. The result seems to justify the computation of the spectral data using the truncated series.

Based on Eq. (33), and using a shell surface absorption coefficient $\alpha = 0.01$, the mean pressure spectra inside the cylindrical shell 1 is plotted in Fig. 8. Since the mean pressure spectrum in the shell enclosure is inversely proportional to the absorption coefficient, any change of the coefficient will be reflected in the pressure spectrum. As it is, the average pressure input to shell external surface is $\frac{1}{4}$psi^2/Hz. Figure 8 indicates that a substantial attenuation (reduction) of pressure spectral density takes place across the vibrating shell.

References

[1] Rice, S. O., "Mathematical Analysis of Random Noises," *Bell System Technical Journal*, Vol. 23, 1944, p. 282; also Vol. 24, 1945, p. 46.

[2] Powell, A., "On Structural Vibration Excited by Random Pressures, With Reference to Structural Fatigue and Boundary Layer Noises," Report SM-22795, May 1957, Santa Monica Div., Douglas Aircraft Co.

[3] Powell, A., "On the Response of Structures to Random Pressures and to Jet Noise in Particular," *Random Vibration*, edited by S. H. Crandall, Wiley, New York, 1958, Chap. 8, pp. 187–229.

[4] Manning, J. E. and Maidanik, G., "Radiation Properties of Cylindrical Shells," *Journal of the Acoustical Society of America*, Vol. 36, No. 9, Sept. 1964, pp. 1691–1698.

[5] Rattayya, J. V. and Junger, M. C., "Flow Excitation of Cylindrical Shells and Associated Coincidence Effects," *Journal of the Acoustical Society of America*, Vol. 36, No. 5, April 1964, pp. 878–884.

[6] *American Institute of Physics Handbook of Physics*, 2nd ed., McGraw-Hill, New York, 1963, pp. 3.67–3.69.

[7] Vlasov, V. Z., *General Theory of Shells and its Applications in Engineering*, TTF-99, April 1964, NASA, pp. 362.

[8] Morse, P. M., *Vibration and Sound*, 2nd ed., McGraw-Hill, New York, 1948, pp. 294–431.